J Indian Soc Remote Sens
DOI 10.1007/s12524-015-0454-4

RESEARCH ARTICLE

ISRS

# A Method for Automatic Road Extraction of High Resolution SAR Imagery

**M. Saati · J. Amini · M. Maboudi**

Received: 13 November 2014 / Accepted: 4 February 2015


**Abstract** Nowadays automatic road extraction from satellite imageries is considered as one of the most important research trends in the field of remote sensing. This paper presents a method for automatic extraction of road centerlines from synthetic aperture radar (SAR) imagery. During the first step, three features, namely the direction of the least total radiance, the corresponding radiance, and the contrast are extracted to define the road characteristics by the backscatter coefficient of each pixel and its neighboring pixels from the SAR imagery. The fusion of the extracted features is carried out in the next step for detection of the road areas by using a fuzzy inference system. Afterwards, the morphology skeletonization is applied on the road areas to extract the road skeleton. Then some interested seed points are extracted so that they could be used in a snake model, which is employed to connect the seed points in order to form up the road centerlines. The proposed algorithm is tested on different parts of TerraSAR-X images. The experimental results reveal that the proposed method is effective in terms of correctness, completeness, and quality.

**Keywords** Road extraction · Fuzzy algorithm · High resolution · Synthetic aperture radar · Active contour model

M. Saati · J. Amini (✉)
Department of Surveying and Geomatics Engineering, College of Engineering, University of Tehran, Kargar-e- Shomali St., Tehran, Iran
e-mail: jamini@ut.ac.ir

M. Saati
e-mail: msaati@ut.ac.ir

M. Maboudi
Islamic Azad University, Qazvin Branch, Qazvin, Iran

## Introduction

Manual extraction of the objects through the satellite imagery done by expert operators is claimed to be really costly and time consuming. Therefore, automatic extraction of the objects from the images is considered as a fundamental research area in the context of remote sensing for mapping applications. Of those objects of interest, roads have been the most frequently appeared objects in the establishment of maps in urban and sub urban areas (Zarrinpanjeh et al. 2013).

When disaster strikes, roads play pivotal roles in bringing relief provisions to the disaster-struck areas. Subsequently, road obstruction information would be necessary for the prompt delivery of the aids. Unfortunately, it is very common that obtaining adequate optical images would be difficult due to bad weather conditions (e.g., cloud coverage) and lack of day/night acquisition capability. Several synthetic aperture radar (SAR) sensors can instead provide wide spatial coverage of the earth, as their sensing capability stays intact throughout day/night and in almost any weather condition. Thus, road extraction from SAR images is complementary or even alternative to optical remote sensing images.

Currently, automatic road extraction from high resolution (HR) SAR data is a high profile research topic. Yet, the complexity involved with extraction increases by the enhanced resolution caused by a phenomenon called the speckle noise. The speckle is an inherent characteristic of the SAR images and is caused by the interferences of waves reflected by many elementary reflectors inside a resolution cell. The speckle causes the neighboring pixels to have considerably different values and thus the speckle has to be removed at the expense of the resolution. Also, the fact that buildings constructed along the roads may obscure the road or reduce its visibility further complicates the road detection. Nowadays, some Earth Observation SAR satellites such as TerraSAR-X, RADARSA

Published online: 10 July 2015

T-2 and COSMO/SkyMed-4, which have operated since 21 June 2010, 14 December 2007, and 5 November 2010 respectively, provide an appropriate resolution in the spotlight mode for the extraction of the roads even in the urban areas (Roth 2003; Lisini et al. 2011).

Plenty of studies have been performed dealing with this issue since the 1990's (Henderson and Xia 1997; Caltagirone et al. 1998). For example, using Markov random field, an early automatic detection algorithm was proposed by (Tupin et al. 1998) for the linear feature extraction such as the main axes of road networks. Moreover, Jeon et al. (2002) developed a technique for the detection of roads in a SAR image using a genetic algorithm.

Based on the Markov random field, Tupin et al. (2002) presented a technique for the detection of roads in dense urban areas using the SAR imagery with different flight directions (orthogonal and anti-parallel passes). Dell'Acqua et al. (2003a) presented an algorithm for the road extraction based on multiple road detectors and logical feature fusion in fine resolution SAR imageries. Wessel (2004) also studied the automatic road extraction from the airborne SAR imagery supported by contextual information. Furthermore, Lisini et al. (2006) presented a road extraction method comprising fusion of classification results and structural information in form of segmented lines. This approach was tested on airborne SAR data of resolution better than 1 m.

Some other researchers have used polarization data for the road extraction. For example, in order to improve the performance of road extractors on SAR images, Zhou et al. (2011) made use of full polarimetric SAR data which measures a target's reflectivity. In addition, Li et al. (2008) presented a road extraction method by high-resolution dual-polarization SAR data over urban areas based on two road detectors at feature-level fusion.

The Bayesian network is also considered as another strategy for refining the road detection algorithms. Stilla and Hedman (2010) used a Bayesian network for the roads extraction from the SAR imagery. In a Bayesian tracking framework, Chen et al. (2005) applied particle filtering in tracking successive road segments.

Hedman et al. (2010) proposed a combination of two road extractors from very high resolution SAR scenes: one more successful in rural areas and the other designed for urban areas. In order to get the best combination of the both, they used a rapid mapping filter for discrimination of rural and urban scenes.

Bentabet et al. (2003) updated road vectors by using the SAR imagery without human–computer intervention, with comprehensive knowledge provided by the road database.

Butenuth and Heipke (2012) presented a network snakes model by bridging the gap between the low-level feature extraction/segmentation and the high-level geometric representation of the objects. They updated the road vectors by using the airborne SAR image as well as the existing road database which was used as the initial value for each snake.

Liu et al. (2013) presented a road extraction method from the SAR imagery based on an improved particle filtering and a snake model.

By in depth analysis of the road detection literature such as (Bentabet et al. 2003; Ravanbakhsh et al. 2008; Butenuth and Heipke 2012), the snake localization in particular, we designed our proposed method to overcome some of the issues reported by the mentioned researches. In our algorithm, in order to overcome the problems associated with the methods using the snake algorithm, among which requiring initial points and computing the external/image energy, we primarily extracted the road regions. Subsequently, the road seed points were selected and used as the initial points in the snake model by applying the morphology skeleton operator on the extracted road regions. Later on, we used our snake model to vectorize the skeleton extracted from the road regions.

It needs to be accentuated that the roads might be more precisely modeled as dark elongated areas surrounded by bright edges particularly in meter or sub-meter SAR spatial resolutions. This would be the case because of double-bounce reflections by the surrounding buildings or uniform backscattering by the vegetation. In this paper, we propose a road region extraction procedure on the basis of a paper published by Negri et al. (2006) for the high-resolution SAR data. The difference, yet, is that in our paper we used a fuzzy inference system (FIS), instead of the logical AND, for the fusion of the extracted features.

## Materials and Methods

As mentioned in the previous section, each snake needs initial values while the binary threshold values have to be known in order to fuse the features together. To solve such issues, namely the fusion of the features for the road region extraction as well as the selection of initial seed points, this study proposes an FIS and a snake model with the purpose of establishing a new process which is potent of yielding a higher performance. In general, the proposed method in this paper can be divided into two stages, as depicted in Fig. 1: road area detection, and vectorization.

In stage 1, or road area detection, the features correspond to road properties in the high resolution SAR imagery are extracted and fused based on a fuzzy algorithm to detect the road areas. Then the spatial and spectral criteria are used for the refinement of the extracted roads (Section 2.1).

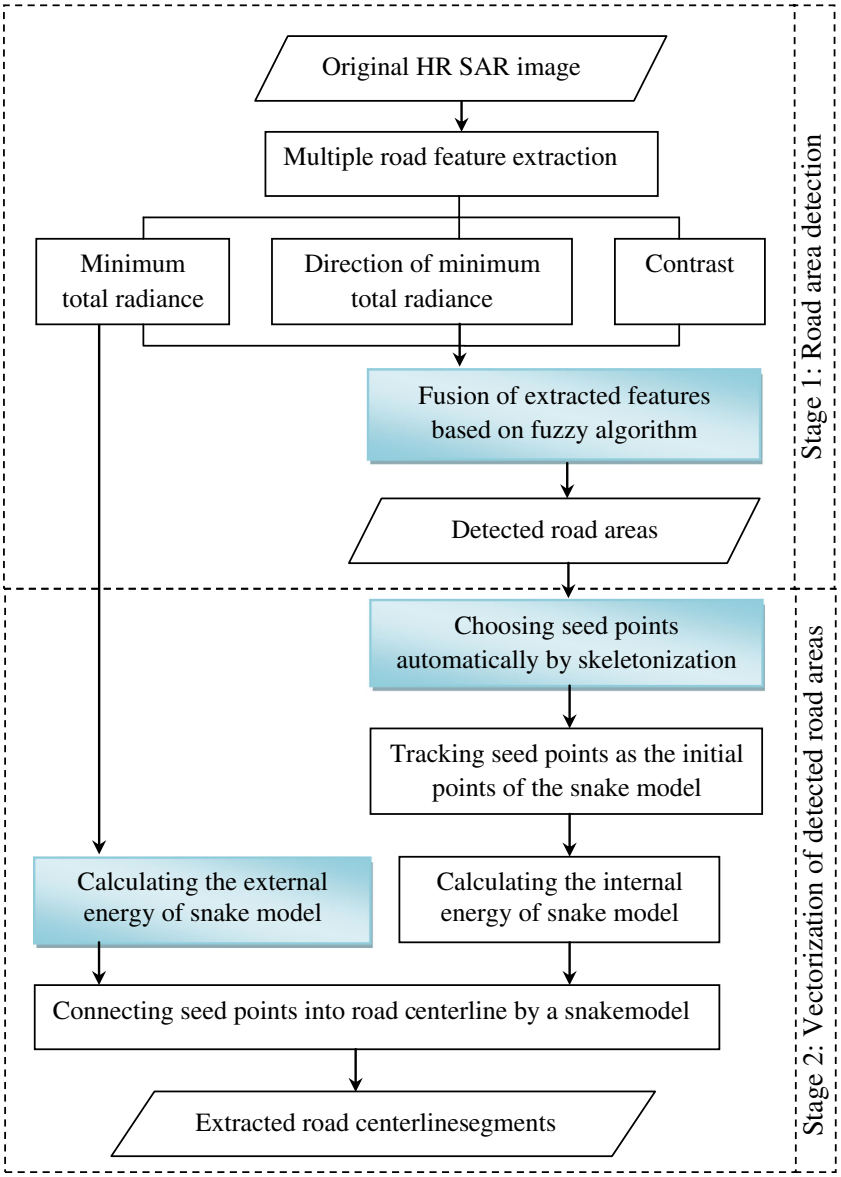


**Fig. 1** The conceptual workflow of the proposed method

In stage 2, or vectorization, many seed points are automatically selected by applying the skeleton operator. Then the road centerlines are extracted by tracking the seed points as the initial points, calculating the internal and external energy for each road centerline segment, and minimizing the total energy of the snake model (Section 2.2).

As the highlighted areas in Fig. 1 depict, there are three important tasks in the proposed method (denoted by a colored background in Fig. 1).

- *Fusion of the extracted features based on a fuzzy algorithm*

  The road candidate extraction in the high-resolution imagery typically starts with the road area detection. In this paper, we assumed that these features were properly chosen and the enhancement was required to be on the fusion method. Looking for straight features in the image and the combination of multiple detectors to improve the road candidate detection, our algorithm exploits spatial and spectral relationships between a pixel and its neighbors. This strategy follows the achievements of (Huber and Lang 2001; Dell'Acqua et al. 2003b; Negri et al. 2006), where multiple detectors were combined by a fuzzy method for higher efficiency. Section 2.1 will further elaborate on the details of this algorithm.

- *Automatically choosing the seed points by skeletonization*

  In order to form a smooth and seamless road, the seed points have to be connected to each other. Since the snake model connects the seed points obtained from skeletonization of the detected road regions, manual selection of the initial points is not necessary.

- *Calculating the external energy of the snake model*
  According to Canny operator, a good edge detector has to maximize the signal-to-noise ratio, the localization, and the multiple-response criterion (McIlhagga 2011). The speckle noise complicates the edge map and external energy calculation. In order to overcome the speckle noise; we use the gradient image of the first extracted feature called the "minimum total radiance" as a measure of the model's external energy. The details are presented in Section 2.2.

In the following sub-sections, we will illustrate the stage of the proposed method in details.

## Road Area Detection

In this paper, multiple detectors have been preferred over a single detector. Thus, straight linear features of the image are investigated considering the spatial and spectral relationship between each pixel and its neighbors. In the next step, the road segment detection is improved by the fuzzy combination of the results derived from different detectors.

As mentioned at an earlier point, the roads appear as extended dark areas with relatively light edges in the high resolution SAR imagery (Negri et al. 2006). Therefore, one should search for pairs with parallel edges, homogeneous areas, and extended dark areas. It is clear that each of the following conditions may per se generate undesirable results. Thus, the solution could be only provided by the combination of the above mentioned conditions and conceptions.

### *Multiple Features Extraction*

For the extraction of pixels of a road, the first step is to calculate some spatial features in a square window around the central pixel p (i, j). However, each of these features will be a function of the window size ($R \times R$). Figure 2 depicts how to select the neighboring pixels of pixel p (i, j) on the image.

As displayed in Fig. 2, the sum of the radiance in a specific direction of $\theta$ in the selected window is called the total radiance and it can be given as (Negri et al. 2006):

$$\boldsymbol{r}(\mathbf{i},\mathbf{j},\mathbf{R},\theta) = \sum_{\mathbf{k}=-\mathbf{R}/2}^{\mathbf{k}=\mathbf{R}/2} \mathbf{p}([\mathbf{i}+\mathbf{k}\cos(\theta)],[\mathbf{j}+\mathbf{k}\sin(\theta)]) \quad (1)$$

Direction of the least total radiance as the first feature is defined as:

$$\boldsymbol{\theta}_0(\boldsymbol{i},\boldsymbol{j},\boldsymbol{R}) = \arg\min_{\theta} \boldsymbol{r}(\boldsymbol{i},\boldsymbol{j},\boldsymbol{R},\boldsymbol{\theta}), \quad \boldsymbol{\theta}\epsilon[0°180°) \quad (2)$$

The corresponding total radiance of $\theta_0$ as the second feature is also defined as:

$$\boldsymbol{r}_0(\mathbf{i},\mathbf{j},\mathbf{R}) = \boldsymbol{r}(\mathbf{i},\mathbf{j},\mathbf{R},\theta_0) \quad (3)$$

$\theta_0$ and $r_0$ demonstrate dark areas elongated around the pixel p(i, j) which is extended in the current window.

Assuming that these areas are candidates for the road, their contrast with the other areas (average total radiance of the other directions) must be high. Therefore, the third feature is the contrast which can be calculated from Eq. (4) as:

$$\boldsymbol{c}_0(\boldsymbol{i},\boldsymbol{j},\boldsymbol{R}) = \left\| \frac{\sum_{\theta} \boldsymbol{r}(\boldsymbol{i},\boldsymbol{j},\boldsymbol{R},\boldsymbol{\theta})}{\mathbf{n}} - \boldsymbol{r}_0(\boldsymbol{i},\boldsymbol{j},\boldsymbol{R}) \right\| \quad (4)$$

Where, $n$ represent the number of the directions for which the value of the total radiance has been calculated.

It is clear that the features $\theta_0$, $r_0$, and $c_0$ display diverse information but they are entirely a function of the window size ($R \times R$); each one might independently reproduce incorrect results which are expected to be deleted through the combining process. What matters here is that the wider and longer road areas will be detected from larger window sizes, whereas the narrow and shorter ones will be characterized by smaller window dimensions.

### *Fuzzy Algorithm*

The road areas in the SAR image is determined by an FIS based on three features: $\theta_0$, $r_0$, and $c_0$. Fuzzy logic provides a simple way to attain a definite conclusion based upon imprecise, uncertain, ambiguous, vague, or missing input information. Introduced by Zadeh (1968), the Fuzzy set theory resembles human reasoning in that it uses approximate information and uncertainty in order to make decisions.

Figure 3 shows the overall flow of the fuzzy algorithm used in this paper.

As seen in the Fig. 3, three linguistic variables namely the least total radiance (LTR), the contrast (Co.), and the direction of the least total radiance (DoLTR) are defined as the input. And also the variable Road is defined as the output of the fuzzy algorithm. Table 1 tabulates the terms of each linguistic variable.

The fuzzy rule base in FIS is based on IF-THEN rules as statements. Generally, a single fuzzy IF-THEN rule can be formulated according to:

IF x is A; THEN y is B.

Where A and B are fuzzy sets defined by the linguistic variable x and y.

For recognizing a road area in HR-SAR images, the fuzzy rule base should include observations of the important features. Some of the fuzzy rules can be listed as follows:

If (Co. is Low) Then (Road is False).
If [(Co. is High) AND (LTR is Low) AND (DoLTR is Moderate)] Then (Road is True).

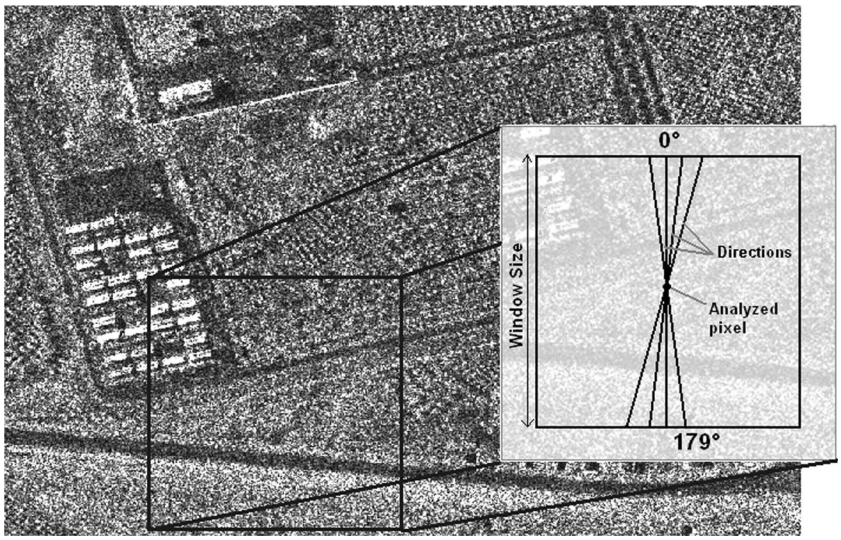


**Fig. 2** Selection of neighborhood pixels

If [(Co. is High) AND (LTR is Middle) AND (DoLTR is Moderate)] Then (Road is Probable) and so on.

Given the rules and input features, the degree of the membership to each of the fuzzy sets has to be determined. Fuzzy processing of the input features requires some specifications of the linguistic variables representing the fuzzy sets. The linguistic variables are listed in Table 1 including three input variables and one output variable along with their fuzzy sets used in the investigation of each extracted feature. The three fuzzy sets are assigned to each input variable, separately. These sets reflect an interactively conducted examination of all possible values associated with the features. In effect, this assignment is mostly a mixture of expert knowledge and examination of the desired input–output data. Moreover, three fuzzy sets are chosen for the linguistic outputs: True, Probably, and False. Also, the most widely applied membership functions are triangular and trapezoidal with a maximum of 1 and a minimum of 0. A sufficient overlap of the neighboring membership functions is taken into account to provide a smooth transition from one linguistic label to another.

Figure 4 shows the process of the FIS. In the first step, the fuzzy AND or OR operators combine the membership values of the input features in each rule which results in one for the antecedent of the same rule. The next step involves the implication of the antecedent to the consequent. Such an implication is carried out for the entire rules. The subsequent step is to aggregate the output fuzzy sets over all the rules. The inputs of the aggregation are the truncated output functions returned by the implication process for each rule. The result of the aggregation process is one fuzzy set per the output variable. What remains in the final step will be used to defuzzify the fuzzy set and to produce a crisp output. The defuzzification method is used to calculate the center of the gravity (centroid) as the crisp value.

As shown in Fig. 4, we follow the Max-Min method (Mamdani and Assilian 1975) in our approach for the FIS because it offers some advantages such as being intuitive, being widely accepted, and being well suited to the human inputs. As an example, assuming three feature values of a pixel: LTR = 0.52, Co. = 0.3 and DoLTR = 0.06 input the system. The process of the fuzzy system is done to calculate the fuzzy resonance result.

Figure 4 exhibits that the pixel is "Road" and the corresponding defuzzified value is equal to 0.903. For a comprehensive study of fuzzy logic and FIS systems, the readers are encouraged to study Zimmermann (2001).

*Refinementation*

The last step of the road detection algorithm is selection of proper road areas on the result image. For this purpose, two criteria are utilized, namely the spatial criteria and spectral criteria.

*The Spatial Criterion* Depending on the ground spatial resolution of the sensors, some of the small detected areas cannot be as a part of the roads network and are ignored accordingly

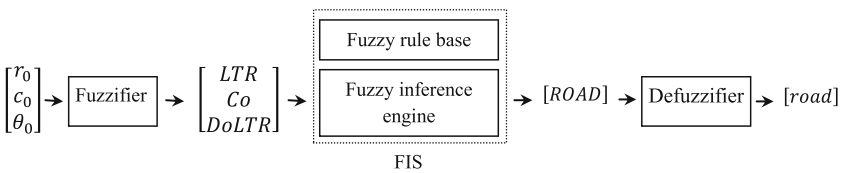


**Fig. 3** The overall flow of the fuzzy algorithm

**Table 1** Linguistic variables and labels for the FIS

| | Linguistic variables | Linguistic labels | Type | Range | Parameters |
|---|---|---|---|---|---|
| Input | Contrast | Low | Trapmf* | [0 1] | [−0.1 0 0.2 0.3] |
| | | Middle | Trimf** | [0 1] | [0.25 0.35 0.45] |
| | | High | Trapmf | [0 1] | [0.4 0.5 1 1.1] |
| | LTR | Low | Trapmf | [0 1] | [−0.1 0 0.4 0.55] |
| | | Middle | Trimf | [0 1] | [0.5 0.65 0.8] |
| | | High | Trapmf | [0 1] | [0.7 0.85 1 1.1] |
| | DoLTR | Close to local average | Trapmf | [0 1] | [−0.1 0 0.05 0.0625] |
| | | Moderate | Trimf | [0 1] | [0.058 0.1 0.2] |
| | | Far to local average | Trapmf | [0 1] | [0.15 0.25 1 1.1] |
| Output | Road | True | Trimf | [0 1] | [−0.1 0 0.5] |
| | | Probably | Trimf | [0 1] | [0.4 0.65 0.8] |
| | | False | Trimf | [0 1] | [0.7 1 1.1] |

*Trapezoidal membership function

**Triangular membership function

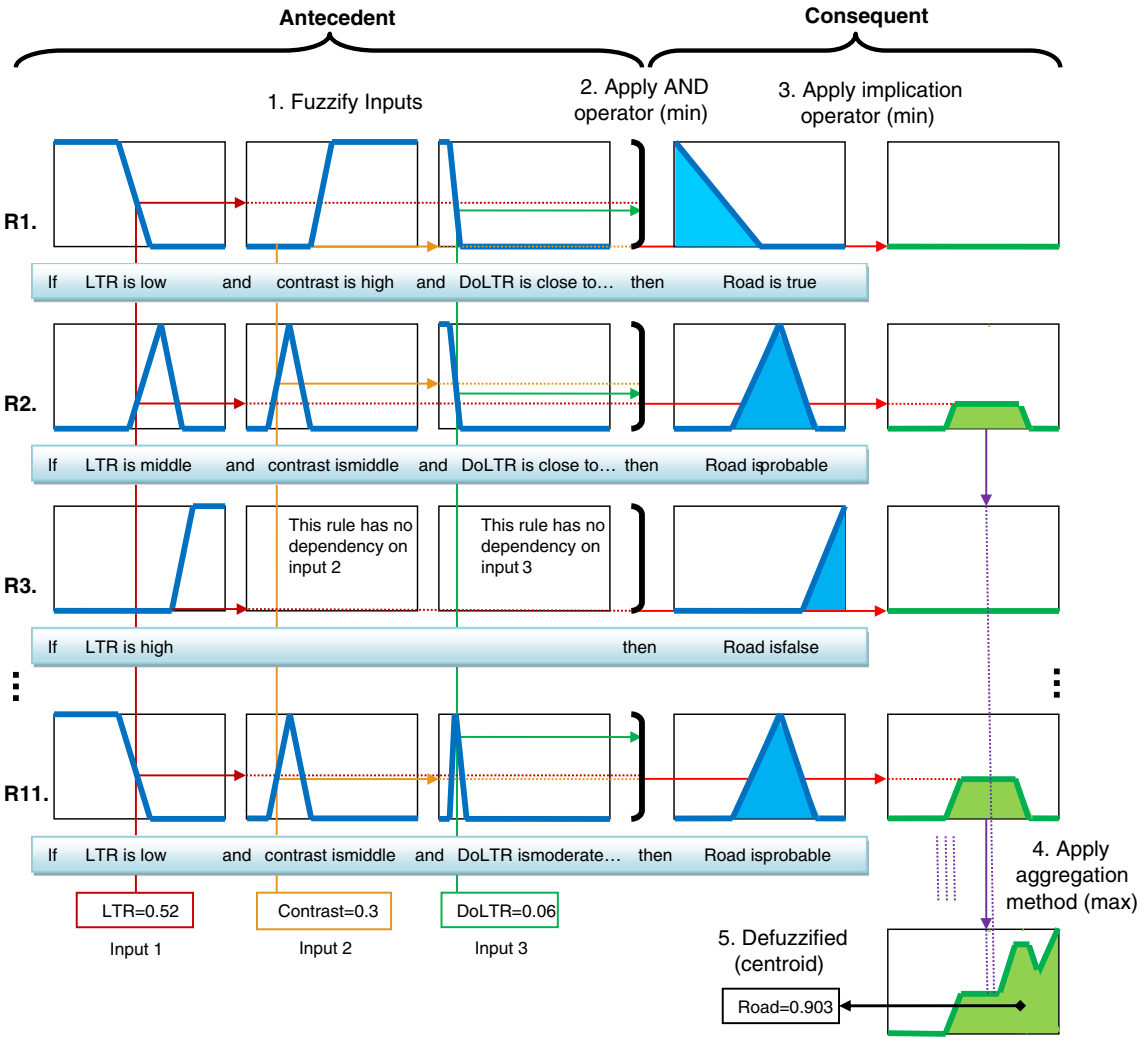


**Fig. 4** FIS scheme of our approach

as they are insignificant. To fulfill such an aim, the areas containing 40 pixels or less can be deleted from the road areas.

*The Spectral Criterion* Considering the average total radiance of the image, the areas detected with very high average radiance cannot be as a part of the roads network. In other words, the areas with average radiance greater than a fraction of the average total radiance are deleted.

### Vectorization of Extracted Road Skeletons

By and large, the active contour model (also known as the snakes) is an energy-minimizing spline guided by external constraint forces and is influenced by image forces pulling it towards the features such as lines and edges (Kass et al. 1988). The snakes are especially useful for delineating the objects that are hard to be modeled with rigid geometric primitives. Since the road centerlines are commonly constructed from diverse shapes having different degrees of curvature, the snakes are well suited in delineating the roads. The traditional parametric active contour, often called a *snake*, is defined as a parametric curve v(s) = [x(s), y(s)], $s\varepsilon[0, 1]$ that moves through the spatial domain of an image to minimize the energy function as (Xu and Prince 1998; Butenuth and Heipke 2012):

$$E_{Snake} = \int_0^1 (E_{int}(v(s)) + E_{ext}(v(s)))ds \quad (5)$$

Where, $E_{int}$ denotes the internal spline energy that controls the features of the snake model. The internal energy includes the parameters of a contour's behavior, such as smoothness and bending. The general formula of $E_{int}$ is defined as:

$$E_{int}(\vec{v}) = \frac{1}{2}\int_0^1 \left(\alpha(s)\left|\frac{\partial \vec{v}(s)}{\partial s}\right|^2 + \beta(s)\left|\frac{\partial^2 \vec{v}(s)}{\partial s^2}\right|^2\right)ds \quad (6)$$

$\alpha(s)$ signifies a measure of the snake's elasticity, controlling the continuity (string forces).

$\beta(s)$ stands for a measure of the snake's stiffness to control the smoothness (rod forces).

The external energy, $E_{ext}$, is derived from the image, which sin turn called *image energy*. It takes on the smallest values at features of interest, such as the boundaries. $E_{ext}$ has no uniform formula and must be defined in accordance with the problem being solved. In the simplest way, the image energy can be expressed by the image intensity. For example, when the object of interest is characterized by the edges, the image energy can be defined as (Butenuth and Heipke 2012):

$$E_{ext}(i, j) = -|\nabla(I(v(s)))|^2 \quad (7)$$

Where $|\nabla(I)|$is the norm or magnitude of the gradient image at the coordinates *x* and y.

To reduce the human–computer interaction, the results of skeletonization of the extracted road regions can be regarded as the initial control points for the snake model. These points converge on the optimal location through internal constraint forces and external image forces. A gradient operator is ordinarily applied for calculating the external energy, and a Gaussian filter is used to reduce the noise before calculating the edge maps. Nonetheless, it needs to be asserted that the gradient operator is not suitable for the signal-dependent multiplicative noise. To ensure the insensitivity of the snake model to speckle as well as guaranteeing that the edge detection would result in good approximation of the road contour, the image energy calculation of the snake model has to be improved. Specifically, the gradient of the *input image* is replaced by that of *the least total radiance image* as:

$$E_{ext}(i, j) = -|\nabla(r_0(i, j))|^2 \quad (8)$$

Where $r_0$ is the least total radiance described in Section 2.1.1.

In the proposed method, the initial seed points are automatically obtained by skeletonization of the extracted road regions. Consequently, the additional calculations and human–computer interactions would be no longer necessary.

## Results and Discussion

In the present research, two experimental data subsets with corresponding roads from Google Earth were used (Fig. 5) which had 1 m resolutions and were taken in the spotlight mode having an incidence angle of 35.3 by using the TerraSAR-X sensor on April 17, 2011. These images cover the sparse regions around Jam, Bushehr, Iran and contain straight roads with different widths. In the first image, a complex scene containing many road intersections, buildings, and trees is presented where as the second one shows a relatively "clean" area.

### Road Area Detection

In the first stage, the features were obtained using the concept presented in Sections 2.1.1 and 2.1.2 by considering the best possible window size. Then the image related to each feature were used as the input to the FIS while the detected road areas would produce the output image. Finally, the defuzzification stage was used in the model to assign the expected (crisp) value for the output image. Figure 6a–c exhibits the feature images for $r_0$, $\theta_0$ and $c_0$ respectively while Fig. 6d indicates the result of FIS fusion of the features. According to Fig. 6d, the dark pixels represent the candidate areas for the road, while the grey pixels show the areas which might be roads,

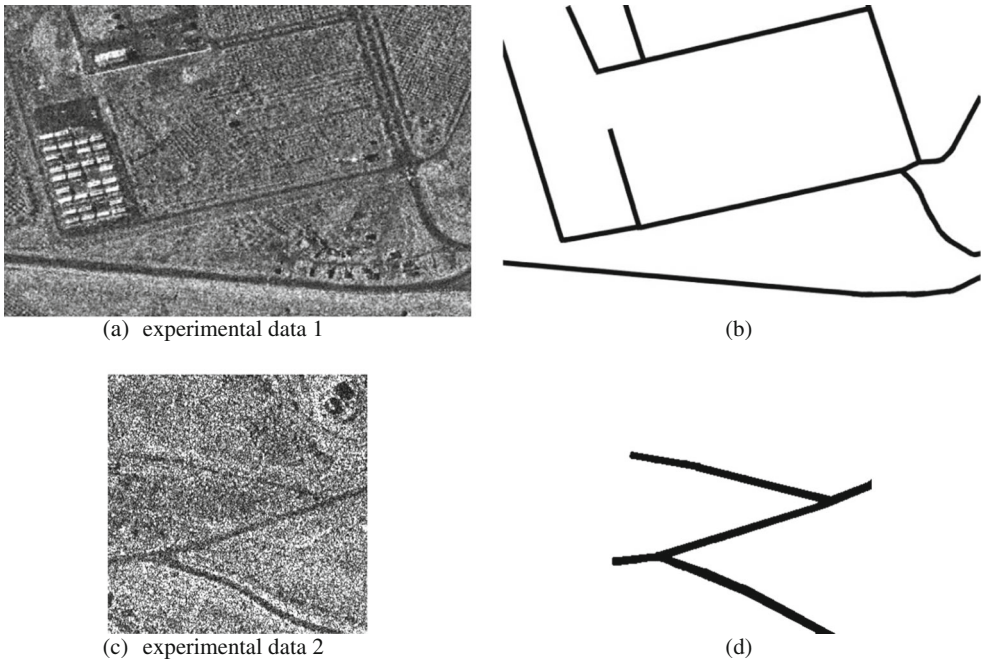

(a) experimental data 1 (b) (c) experimental data 2 (d)

**Fig. 5** The experimental data. **a**, **c** are two TerraSAR-X images with 1 m resolution. **b**, **d** are Corresponding road data from Google Earth™

and the light pixels are representative of the background or the non-road areas.

In order to analyze the sensitivity of the algorithm to the speckle noise as well as the window size, a Gamma-MAP filter was used with a kernel size of 3 by 3 and 5 by 5 pixels in addition to using square windows with variable sizes of 5, 10,15, and 20 pixels, respectively. Because no significant improvement was made in completeness and correctness because by using the "minimum total radiance" feature in the road area detection stage instead of the alone pixel, the information of the neighbor pixels was used and the average operation reduced the effect of the speckle noise on our algorithm. It was concluded that the abovementioned algorithm had no sensitivity to the existing speckle noise in the SAR images. Furthermore, using a larger window size made it possible to detect the wider and longer road areas.

Later on, spectral and spatial criteria were separately applied to the image in order to improve the performance. Thereby, those regions with an average radiance greater than 70 % of the average radiance of the images or the regions with an area smaller than 40 pixels were dismissed from the detected road areas.

Analyzing the numerical accuracy revealed that the sensitivity of the mentioned algorithm had been mainly focused on

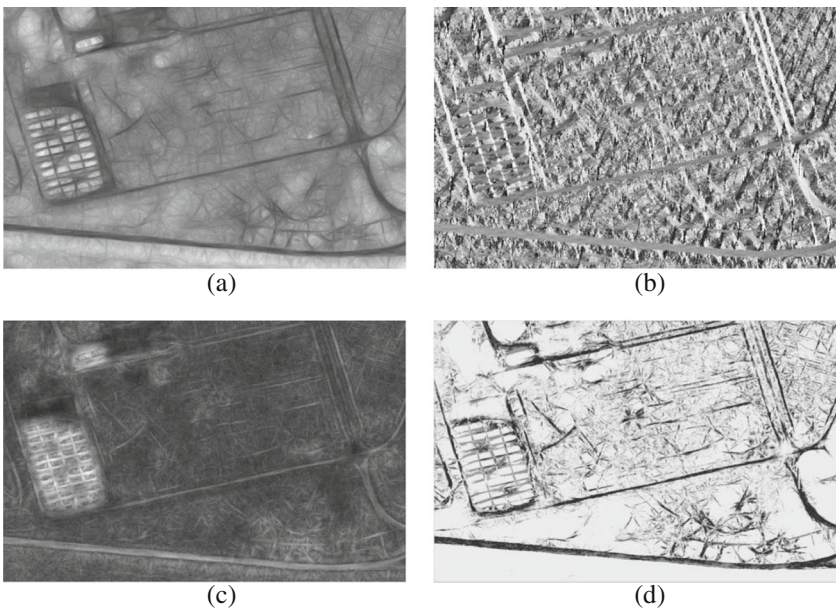

(a) (b) (c) (d)

**Fig. 6** **a**, **b** and **c** are images of extracted features related to $r_0$, $\theta_0$ and $c_0$ respectively and **d** is image of features fusion

**Table 2** Quantitative evaluation of the proposed method

| Method | Experimental data | Reference map | Completeness | Correctness | Quality |
|---|---|---|---|---|---|
| Proposed method | 1 | Fig. 5b | 82 % | 50 % | 45 % |
| Negri's method (Negri et al. 2006) | 1 | Fig. 5b | 77 % | 47 % | 43 % |
| Proposed method | 2 | Fig. 5d | 88 % | 72 % | 64 % |

detecting the road areas. Besides, applying the spatial and spectral criteria in choosing the proper road areas will add to that sensitivity. It was observed that the refinement step could only enhance the surrounding areas while no enhancements were practically observed for the detected road areas.

For quantifying the performance values, three accuracy measures proposed by Wiedemann (2003) were considered in order to evaluate the proposed method:

$$\text{Completeness} = \frac{\text{TP}}{(\text{TP} + \text{TN})} \tag{9}$$

$$\text{Correctness} = \frac{\text{PT}}{(\text{PT} + \text{PF})} \tag{10}$$

$$\text{Quality} = \frac{\text{TP}}{((\text{TP} + \text{TN}) + \text{FP})} \tag{11}$$

Where T, F, P and N, mean true, false, positive and negative, respectively.

- TP is the length of the matched extracted data within the buffer around the reference road data,
- PT denotes the length of the matched reference road data within the buffer around the extracted data,
- FP is the length of the unmatched extracted data,
- PF stands for the length of unmatched reference road data, and
- TN is the length of the reference data which is not located within the buffer around the extracted data.

The completeness is the percentage of the reference data which is explained by the buffered extracted data, i.e., the percentage of the reference network which could be extracted. It needs to be accentuated that the optimum values for the completeness and correctness would be 1.

The correctness represents the percentage of the correctly extracted road data, i.e., the percentage of the extraction, which is in accordance with the buffered reference. The optimum value for the correctness is 1 while the buffer width was set to 10 m in this study. The comparison results are presented in Table 2.

The quantitative evaluation results tabulated in Table 2 indicate that the proposed method successfully distinguished the main roads from the high resolution SAR imagery. However, Table 2 also represents that the completeness in experimental data 2 is much higher than that of experimental data 1. This is mainly because the spatial pattern in experimental data 1 is more complicated than that of experimental data 2.

As expected, the roads parallel to the incident direction were much more visible than the others. In very dense urban areas, layover and shadowing effects of the SAR data makes nearly half of the road network invisible (Tupin et al. 2002).

As shown in Fig. 7, the areas marked with tag B (blue area) are wrongly detected as road areas due to the following reasons:

- The shadow of regularly distributed rows of trees
- Tracing areas caused by agricultural machineries footprints, or
- Road areas that are not labeled as road areas by Google Earth™, i.e. Blvd. roads are considered as single roads.

Furthermore, the algorithm was unable to detect the areas marked with tag R (red area) due to one of these reasons:

- Areas without sufficiently high contrast in comparison with their surroundings,
- Areas completely covered by adjacent trees, or
- Areas located at margins of the image.

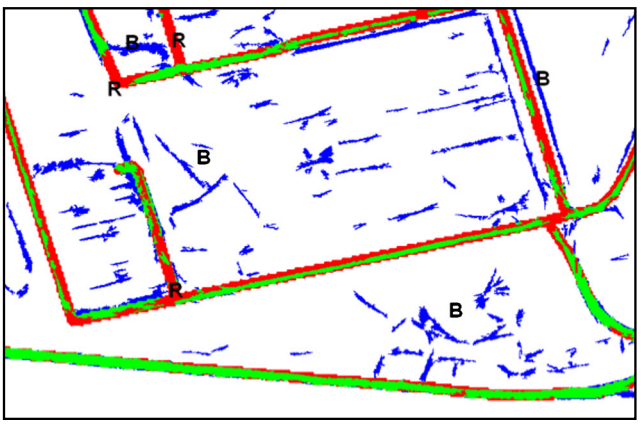


**Fig. 7** Image of the detected areas (*green*: correctly detected areas, *blue*: incorrectly detected areas, *red*: undetected areas, *white*: non-road areas)

(a) (b)

**Fig. 8** **a** the road extraction result of the experimental data 1 by the snake model, **b** the road extraction result superimposed on original image

The snake model was used for vectorization of the extracted road regions. Traditional snakes are sensitive to the noise and need a precise initialization. In order to solve this issue, the gradient image of the least total radiance is used instead of the gradient image. Also, for precise initializing, the skeletonization of the extracted road regions is performed to find the road centerline segment and then the interest seed points were automatically selected over these segments. The seed points consisted of head, tail, and constant inter spaces for each segment. Moreover, in this study $\alpha$ and $\beta$ parameters were tuned to be 0.1 and 0.9, respectively. The results of the vectorization stage over the experimental data set 1 and 2 are respectively illustrated in Figs. 8 and 9. The red lines in these Figures represent the road extracted by the proposed method.

## Conclusions

Extraction of the roads from high resolution optical and SAR images has already extended the horizon of the applications in which such images are being used. This paper proposed a method for road centerline extraction from the high resolution SAR images. The areas earmarked as "would-be" roads were obtained in this study by three features extracted based on the difference between the road pixels in comparison with their surroundings and then fusing them together into a fuzzy algorithm. The obtained results indicated the algorithm success in detection of the road areas compared to the threshold-based method (i.e. the logical AND operator in the method of Negri et al. (2006)), as well as the insensitivity to the speckle noise. Eventually, by applying an improved snake model without human contribution, the detected road skeletons were vectorized and the road centerlines were extracted precisely. The experimental results for the SAR image suggested that the main roads in the images could be accurately located and extracted. Moreover, the presented method considerably boosted up the efficiency as well as the practicality. Nonetheless, it has been noticed that the proposed method could be improved by considering the topological relations when extracting the complex road network seven though the proposed method could be used to extract a single road or several roads in SAR imagery.

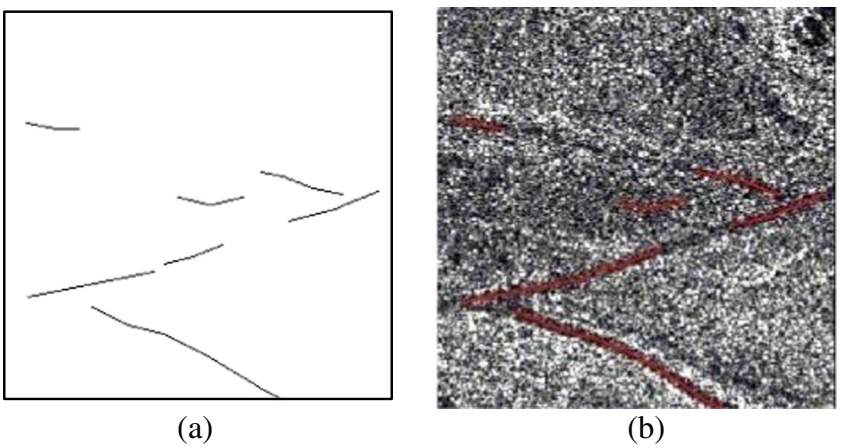

(a) (b)

**Fig. 9** **a** the road extraction result of the experimental data 2 by the snake model, **b** the road extraction result superimposed on original image

## References


Bentabet L., Jodouin S., Ziou D., & Vaillancourt J. (2003). Road vectors update using SAR imagery: a snake-based method. *IEEE Transactions on Geoscience and Remote Sensing*, *41*(8), 1785–1803.

Butenuth M., & Heipke C. (2012). Network snakes: graph-based object delineation with active contour models. *Machine Vision and Applications*, *23*(1), 91–109.

Caltagirone, F., Spera, P., Vigliotti, R., & Manoni, G. (1998). SkyMed/COSMO mission overview. In *Geoscience and remote sensing symposium proceedings, 1998. IGARSS'98. 1998 I.E. International, 1998* (Vol. 2, pp. 683–685). IEEE.

Chen, Y., Gu, Y., Gu, J., & Yang, J. (2005). Particle filter based road detection in SAR image. In *Microwave, antenna, propagation and EMC technologies for wireless communications, 2005. MAPE 2005. IEEE International Symposium on, 2005* (Vol. 1, pp. 301–305). IEEE.

Dell'Acqua F., Gamba P., & Lisini G. (2003a). Improvements to urban area characterization using multitemporal and multiangle SAR images. *IEEE Transactions on Geoscience and Remote Sensing*, *41*(9), 1996–2004.

Dell'Acqua F., Gamba P., & Lisini G. (2003b). Road map extraction by multiple detectors in fine spatial resolution SAR data1. *Canadian Journal of Remote Sensing*, *29*(4), 481–490.

Hedman K., Stilla U., Lisini G., & Gamba P. (2010). Road network extraction in VHR SAR images of urban and suburban areas by means of class-aided feature-level fusion. *IEEE Transactions on Geoscience and Remote Sensing*, *48*(3), 1294–1296.

Henderson F. M., & Xia Z.-G. (1997). SAR applications in human settlement detection, population estimation and urban land use pattern analysis: a status report. *IEEE Transactions on Geoscience and Remote Sensing*, *35*(1), 79–85.

Huber, R., & Lang, K. (2001). Road extraction from high-resolution airborne SAR using operator fusion. In *Geoscience and Remote Sensing Symposium, 2001. IGARSS'01. IEEE 2001 International, 2001* (Vol. 6, pp. 2813–2815). IEEE.

Jeon B.-K., Jang J.-H., & Hong K.-S. (2002). Road detection in spaceborne SAR images using a genetic algorithm. *IEEE Transactions on Geoscience and Remote Sensing*, *40*(1), 22–29.

Kass M., Witkin A., & Terzopoulos D. (1988). Snakes: active contour models. *International Journal of Computer Vision*, *1*(4), 321–331.

Li, S.-y., Yang, W., Yang, H., & Sun, H. (2008). Road extraction from high resolution dual-polarization SAR images over urban areas. In *International Conference on Earth Observation Data Processing and Analysis, 2008* (pp. 72850Q-72850Q-72810). International Society for Optics and Photonics.

Lisini G., Tison C., Tupin F., & Gamba P. (2006). Feature fusion to improve road network extraction in high-resolution SAR images. *IEEE Geoscience and Remote Sensing Letters*, *3*(2), 217–221.

Lisini G., Gamba P., Dell'Acqua F., & Holecz F. (2011). First results on road network extraction and fusion on optical and SAR images using a multi-scale adaptive approach. *International Journal of Image and Data Fusion*, *2*(4), 363–375.

Liu J., Sui H., Tao M., Sun K., & Mei X. (2013). Road extraction from SAR imagery based on an improved particle filtering and snake model. *International Journal of Remote Sensing*, *34*(22), 8199–8214. doi:10.1080/01431161.2013.835082.

Mamdani, E. H., & Assilian, S. (1975). An experiment in linguistic synthesis with a fuzzy logic controller. International Journal of Man-Machine Studies, 7(1), 1–13.

McIlhagga W. (2011). The Canny edge detector revisited. *International Journal of Computer Vision*, *91*(3), 251–261.

Negri M., Gamba P., Lisini G., & Tupin F. (2006). Junction-aware extraction and regularization of urban road networks in high-resolution SAR images. *IEEE Transactions on Geoscience and Remote Sensing*, *44*(10), 2962–2971.

Ravanbakhsh M., Heipke C., & Pakzad K. (2008). Road junction extraction from high-resolution aerial imagery. *The Photogrammetric Record*, *23*(124), 405–423.

Roth, A. (2003). TerraSAR-X: a new perspective for scientific use of high resolution spaceborne SAR data. In *Remote Sensing and Data Fusion over Urban Areas, 2003. 2nd GRSS/ISPRS Joint Workshop on, 22–23 May 2003* (pp. 4–7). doi:10.1109/dfua.2003.1219947.

Stilla, U., & Hedman, K. (2010). Feature fusion based on bayesian network theory for automatic road extraction. In *Radar Remote Sensing of Urban Areas* (pp. 69–86). Springer.

Tupin F., Maitre H., Mangin J.-F., Nicolas J.-M., & Pechersky E. (1998). Detection of linear features in SAR images: application to road network extraction. *IEEE Transactions on Geoscience and Remote Sensing*, *36*(2), 434–453.

Tupin F., Houshmand B., & Datcu M. (2002). Road detection in dense urban areas using SAR imagery and the usefulness of multiple views. *IEEE Transactions on Geoscience and Remote Sensing*, *40*(11), 2405–2414.

Wessel B. (2004). Road network extraction from SAR imagery supported by context information. *The International Archives of the Photogrammetry, Remote Sensing and Spatial Information Sciences*, *35*, 360–366.

Wiedemann C. (2003). External evaluation of road networks. *The International Archives of the Photogrammetry, Remote Sensing and Spatial Information Sciences*, *34*(3/W8), 93–98.

Xu C., & Prince J. L. (1998). Snakes, shapes, and gradient vector flow. *IEEE Transactions on Image Processing*, *7*(3), 359–369.

Zadeh L. A. (1968). Fuzzy algorithms. *Information and Control*, *12*(2), 94–102.

Zarrinpanjeh N., Samadzadegan F., & Schenk T. (2013). A new ant based distributed framework for urban road map updating from high resolution satellite imagery. *Computers & Geosciences*, *54*, 337–350.

Zhou G., Cui Y., Chen Y., Yang J., Rashvand H., & Yamaguchi Y. (2011). Linear feature detection in polarimetric SAR images. *IEEE Transactions on Geoscience and Remote Sensing*, *49*(4), 1453–1463.

Zimmermann H. J. (2001). *Fuzzy set theory-and its applications*. Springer.